J Appl Electrochem (2008) 38:215–224
DOI 10.1007/s10800-007-9427-9

ORIGINAL PAPER

Influence of cobalt ions on the anodic oxidation of a lead alloy under conditions typical of copper electrowinning

T. Nguyen · N. Guresin · M. Nicol · A. Atrens

Received: 1 June 2007 / Revised: 21 September 2007 / Accepted: 21 September 2007 / Published online: 9 October 2007
© Springer Science+Business Media B.V. 2007

Abstract The influence of cobalt ions in the solution on the anodic oxidation of a commercial Pb–Ca–Sn alloy under conditions typical of copper electrowinning was studied using cyclic voltammograms and potential decay transients. The cobalt ions changed the structure, morphology and chemical composition of the surface film from a loose porous film to a thin dense film. This change of surface film is the cause for the decreased rate of oxidation for the lead anode in the presence of cobalt ions. The steady state potential of the alloy during anodic oxidation decreased with (i) increasing cobalt ion concentration, (ii) increasing rotation speed, (iii) increasing temperature, (iv) decreasing acid concentration and (v) decreasing current density. The steady state potentials were lower in the presence of cobalt ions. This decrease in the steady state potential may indicate that oxygen evolution is more rapid on the more compact film formed in the presence of cobalt ions. Alternatively, an additional pathway of oxidation may be provided by the cobalt ions.

Keywords Lead oxidation · Anodic oxidation · Lead anode · Copper electrowinning · Cyclic voltammetry · Oxygen evolution reaction · Lead dioxide · Passive film

T. Nguyen · N. Guresin · A. Atrens (✉)
School of Engineering, The University of Queensland, Brisbane, QLD 4072, Australia
e-mail: a.atrens@minmet.uq.edu.au

M. Nicol
AJ Parker CRC for Hydrometallurgy, School of Chemical and Mathematical Sciences, Murdoch University, Murdoch, WA 6150, Australia

1 Introduction

For copper electrowinning from sulphuric acid solutions the preferred anode material is a lead–calcium–tin alloy. Its low oxidation rate is attributed to the formation of a protective surface oxide at the high operating potential of about 2 V (SHE). The predominant reaction at the anode is oxygen evolution by Eq. 1. The fresh anode surface is initially covered with a non-conducting layer of $PbSO_4$ formed by reaction (2). $PbSO_4$ is oxidised to the conducting oxide PbO_2 via reaction (3)

$$2H_2O = O_2 + 4H^+ + 4e^- \qquad E = 1.23V \qquad (1)$$

$$Pb + SO_4^{2-} \leftrightarrow PbSO_4 + 2e^- \qquad E = -0.373V \qquad (2)$$

$$PbSO_4 + 2H_2O \leftrightarrow PbO_2 + H_2SO_4 + 2H^+ + 2e^- \quad E = 1.685V \qquad (3)$$

The PbO_2 layer hinders further lead oxidation, but some oxidation occurs by oxidation through the PbO_2 layer or at breaks in the oxide layer.

Prior research [1–18] has shown that a small amount (less than 100 ppm) of cobalt ions in the electrolyte results in a lower oxidation rate of the lead alloy, a lower oxygen overpotential (or at least a lower potential of the lead), a smaller amount of PbO_2 on the lead surface [12] and mainly lead sulphate [19] as the oxidation product. The lower potential at the lead anode could lead directly to a lower oxidation rate. Krivolapova and Kabanov [3] suggested that cobalt decreased lead oxidation by the adsorption of Co^{3+} ions or CoO_2 forming a dense blocking film. Alternatively [4, 5], cobalt ions may provide an oxidation pathway alternate to oxygen evolution; namely

$$Co^{2+}_{(ads)} \rightarrow Co^{3+}_{(ads)} + e \quad (4)$$

Co^{3+} ions can react chemically with water producing oxygen and regenerating Co^{2+} by:

$$4Co^{3+}_{(ads)} + 2H_2O \rightarrow 4Co^{2+}_{(ads)} + 4H^+ + O_2 \quad (5)$$

Although it is well known that the lead oxidation rate is lower with cobalt ions in the solution, the mechanism is not understood. This paper describes research into the influence of cobalt ions on the oxidation of a commercial Pb–Ca–Sn alloy under conditions typical of those used in practice.

2 Experimental

The three-electrode electrochemical cell was a 200 mL water-jacketed glass cell as shown in Fig. 1. The electric motor for the rotating working electrode was mounted directly above the cell. A Luggin capillary was fitted in the bottom of the cell. A platinum wire was the counter electrode. Unless otherwise stated, the electrolyte was a 170 g L^{-1} H_2SO_4 solution. The cobalt ions were added as cobalt sulphate, $CoSO_4 \cdot 7H_2O$. All solutions used AR grade chemicals and distilled water. A Hg|$HgSO_4$| saturated K_2SO_4 reference electrode was used to avoid chloride contamination. The potentials are reported with respect to the standard hydrogen electrode (SHE). The potential of the working electrode was controlled by a PAR 362 potentiostat. The potential and current were logged by a computer using a data acquisition system operated by the Lab VIEW 7 software. All measurements were made at room temperature, except when the influence of temperature was studied.

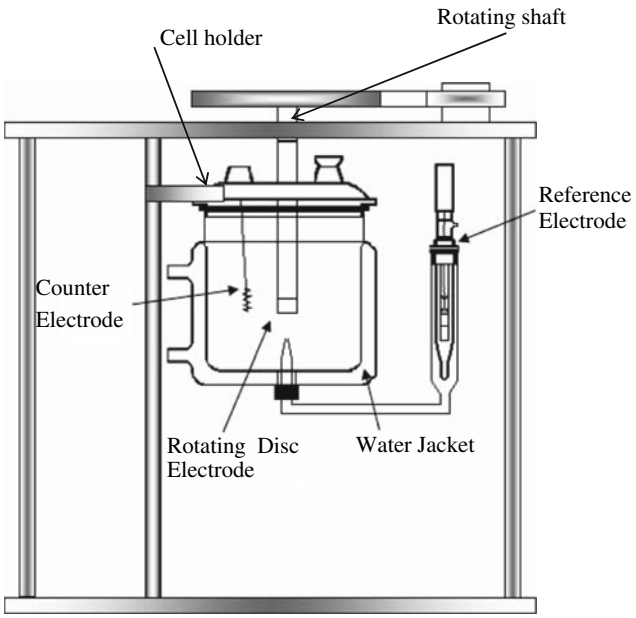

Fig. 1 The electrochemical cell

The working electrode was a cylindrical rotating disc that was embedded in epoxy and was attached to a stainless steel disc using conductive silver-loaded epoxy (Araldite LC 191, Hardener LC 26). The composition of the commercial Pb–Ca–Sn alloy was 1.4%Sn, 0.080% Ca, 0.020% Al and balance Pb. The working electrode stub was screwed into an electrode holder, Fig. 2, to allow the electrode to be unscrewed and placed in a scanning electron microscope (SEM) for analysis. Unless stated otherwise, the electrode was rotated at 500 rpm. Immediately before each experiment, the electrode was polished using 1,200 grit paper and thoroughly rinsed with acetone and distilled water.

The influence of cobalt ions in the solution on the anodic oxidation of the Pb–Ca–Sn alloy was studied using cyclic voltammetry to characterize the oxidation products after oxidation at 285 A m^{-2} for a fixed period. This current density of 285 A m^{-2} reflects a typical value used in industry. Complementary measurements were carried out of the potential decay of electrodes in solutions with and without cobalt ions after oxidation at constant current density.

3 Results

3.1 Typical cyclic voltammogram

Figure 3 presents a typical cyclic voltammogram, measured after the Pb–Ca–Sn alloy had been oxidised for 1 h at 285 A m^{-2} in 170 g L^{-1} H_2SO_4. The voltamogram was measured at a scan rate of 10 mV/s, a scan rate not untypical for such research. The potential during the oxidation was ~2.1 V. During the negative scan from this potential, reduction of PbO_2 to $PbSO_4$ occurs at ~1.55 V (peak C), followed by a small anodic peak D at ~1.45 V, the reduction of PbO to Pb at ~ –0.4 V (peak E), $PbSO_4$ to Pb at –0.45 V (peak F) and the evolution of hydrogen at more negative potentials. The small peak D is due to the oxidation of metallic lead to lead sulfate or oxide [20, 21] in cracks produced in the PbO_2 film during reduction to lead sulfate. On the positive scan from negative potentials, the oxidation of Pb to $PbSO_4$ occurs at approximately –0.3 V.

The quantity of Pb oxidised to PbO_2 during anodic oxidation can be evaluated by integrating the charge under peak C, whilst the total amount of Pb oxidised can be obtained from the area under peaks E and F. This method of evaluation of the oxidation rate assumes that all the

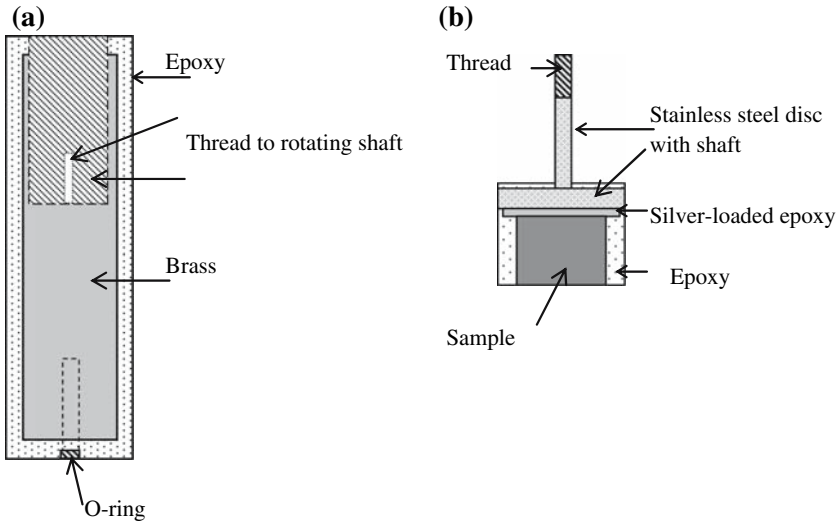

Fig. 2 (**a**) electrode holder and (**b**) electrode stub for SEM studies

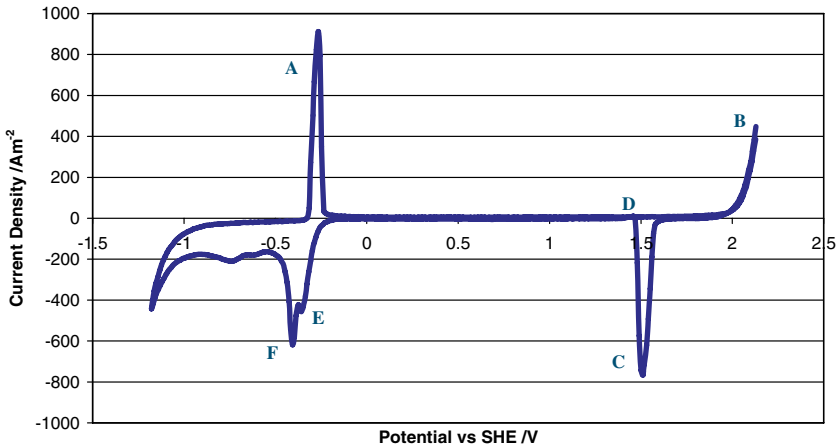

Fig. 3 Typical cyclic voltammogram of a rotating Pb–Ca–Sn electrode after 1 h oxidation at 285 A m^{-2} in 170 g L^{-1} H_2SO_4 at room temperature and at 500 rpm. The potential was swept at 10 mV s^{-1} in a negative direction from the potential at ~2.1 V. Subsequently the positive scan was measured

oxidation products remain on the surface. After each experiment, the solution was carefully examined and there was no evidence of spalling of oxidation products. The oxidation rate is presented as total mass of Pb oxidised by the equation

$$W = \frac{MIt}{nF} \quad (6)$$

where W = weight of the electro-active species (g), M = molecular mass of lead, I = current (A), t = time (s), F = Faraday = 96,480 Coulomb mol^{-1}. The oxidation rate is expressed in units of g Pb $(kAh)^{-1}$.

3.2 Effect of cobalt concentration

The steady-state potential of the Pb–Ca–Sn alloy during the oxidation at 285 A m^{-2} decreased with increasing concentration of cobalt ions in the electrolyte, Fig. 4. This is consistent with prior research [17]. The extent of oxidation (as PbO_2 and total Pb) derived from the voltammograms measured after 1 h, as described above for the experiments shown in Fig. 4, are summarized in Fig. 5. The oxidation rate decreased as the cobalt ion concentration increased from 0 to 500 ppm with the most significant decrease occurring at low cobalt ion concentrations. The amount of PbO_2 on the surface also decreased with increase in cobalt ion concentration. These results agree with prior research [17].

SEM micrographs of the film formed on the Pb–Ca–Sn alloy surface after 1 h of oxidation at 285 A m^{-2} are shown in Fig. 6. The film formed in the absence of cobalt was thick, porous and discontinuous whereas that developed in the presence of 100 ppm Co^{2+} was thin and compact. This suggests that the formation of a continuous and impermeable oxide film in the presence of cobalt ions acts to protect the underlying metal surface. Hrussanova et al [15] speculated that the porous film consisted of β-PbO_2 and the dense part was composed of PbO_t, PbO_x and α-PbO_2 and that the oxidation rate increased with the content of β-PbO_2 in the film.

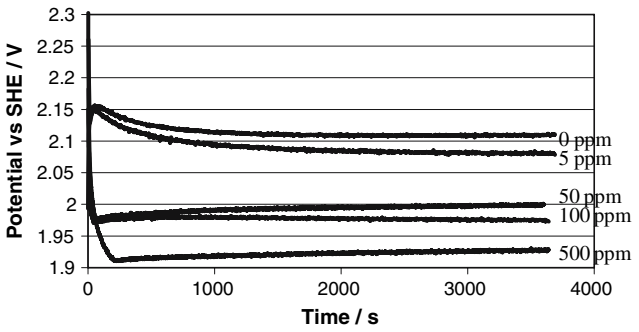

Fig. 4 The influence of cobalt ion concentration on the potential of the Pb–Ca–Sn alloy during oxidation at 285 A m^{-2}

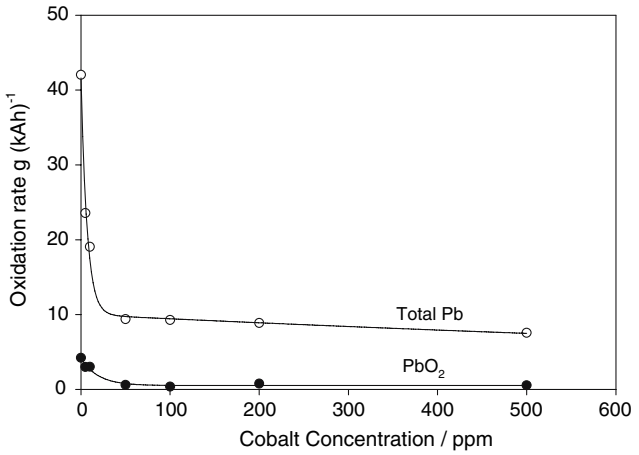

Fig. 5 The effect of cobalt ion concentration on the oxidation rate [expressed as total Pb] and the amount of PbO_2 [expressed as Pb] on the Pb–Ca–Sn alloy after oxidation for 1 h at 285 A m^{-2}

Figure 7 shows that peak E, which is attributed to the reduction of PbO to Pb, was either not present in the anodic film for cobalt concentrations above 10 ppm or PbO was not produced in the reduction of the PbO_2 layer formed in the presence of cobalt ions. This observation is consistent with prior observations [22]. Figure 7 also shows that the amount of $PbSO_4$ on the partially reduced surface was small for cobalt ion concentrations of 50 ppm and above.

3.3 Effect of rotation speed

The influence of electrode rotation speed on the potential of the Pb–Ca–Sn alloy during oxidation at 285 A m^{-2} is presented in Fig. 8. The steady state potential decreased slightly with increasing rotation speed in the absence of cobalt ions. This effect was more pronounced in the presence of cobalt ions. These results suggest that the rate of evolution of oxygen is at least partially controlled by mass transfer of cobalt ions to the anode surface. The steady state potentials were lower in the presence of cobalt ions.

Figure 9 presents the oxidation rate and amount of surface PbO_2 measured after oxidation at various electrode rotation speeds. There was little influence of rotation rate on oxidation rate, whereas the amount of PbO_2 decreased slightly with increasing rotation speed. This was similar to the observations of Velichenko et al. [23]. The oxidation rate and the amount of surface PbO_2 was lower in the presence of cobalt ions.

3.4 Effect of temperature

Figure 10 shows that the steady state potential decreased with increasing temperature and this decrease was lower in the presence of cobalt ions. The steady state potential at 55 °C was about 90 mV lower than that at 25 °C in the absence of cobalt ions, whereas the potential at 55 °C was about 70 mV lower than that at 25 °C in the presence of 100 ppm Co^{2+}. The steady state potentials were lower in the presence of cobalt ions.

Figure 11 presents the influence of temperature on the oxidation rate and amount of surface PbO_2. The oxidation rate and the amount of PbO_2 on the surface increased somewhat with temperature in the absence of cobalt ions. With cobalt ions in the solution, the oxidation rate increased substantially from 25 to 45 °C and the amount of PbO_2 decreased somewhat with increasing temperature. The oxidation rate and the amount of surface PbO_2 were lower in the presence of cobalt ions.

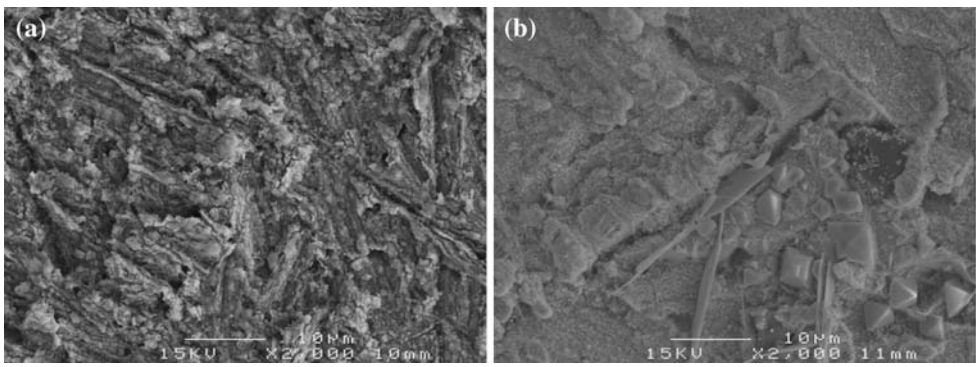

Fig. 6 SEM micrographs of the film formed on the Pb–Ca–Sn alloy after oxidation for 1 h at 285 A m^{-2} in 170 g L^{-1} H_2SO_4 containing (**a**) 0 ppm Co^{2+} and (**b**) 100 ppm Co^{2+}

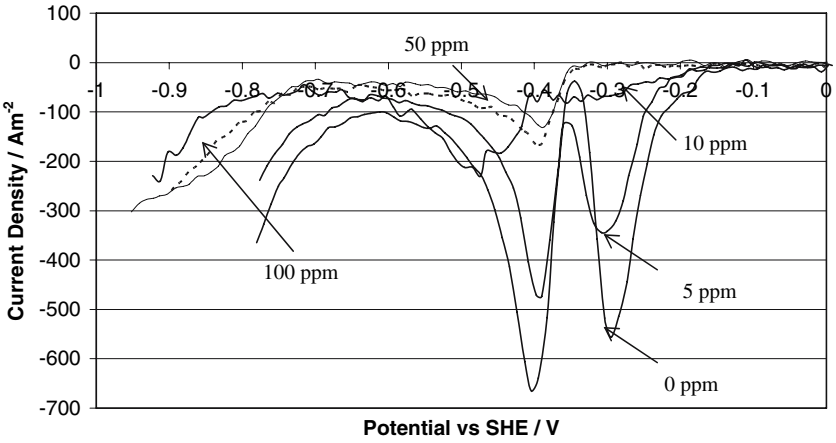

Fig. 7 Potential sweep curves in a negative direction for a rotating Pb–Ca–Sn disc anode after oxidation at 285 A m^{-2} for 1 h in 170 g L^{-1} H_2SO_4 solution and the stated cobalt ion concentration

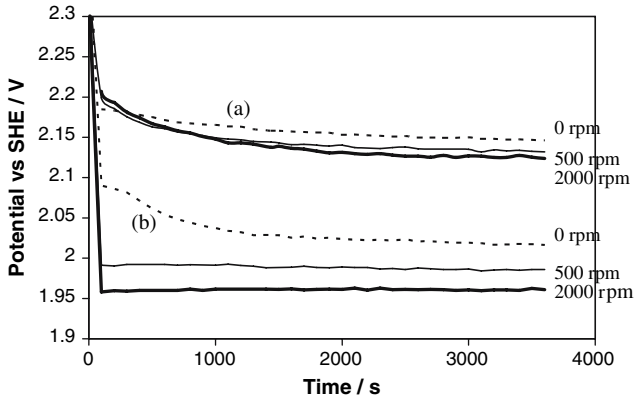

Fig. 8 Effect of electrode rotation speed on the potential of the Pb–Ca–Sn alloy during oxidation at 285 A m^{-2} in 170 g L^{-1} H_2SO_4 containing (**a**) 0 ppm Co^{2+} and (**b**) 100 ppm Co^{2+}

3.5 Effect of acid concentration

The influence of acid concentration on the potential is presented in Fig. 12. The steady state potential in the presence of cobalt ions was lower in all cases. With no cobalt ions in solution, the steady state potential increased by 25 mV as the acid concentration was increased from 100 to 250 g L^{-1} whereas the increase was 100 mV in the presence of cobalt ions.

Figure 13(a) shows that, in the electrolyte with no cobalt, the oxidation rate increased to a maximum as the acid concentration increased from 100 to 170 g L^{-1} and then decreased somewhat as the acid concentration increased further to 250 g L^{-1}; the amount of PbO_2 increased with increased acid concentration. Figure 13(b) shows that, in the electrolyte containing 100 ppm cobalt ions, the oxidation rate and the amount of surface PbO_2 increased slightly. The oxidation rate and the amount of surface PbO_2 were significantly lower in the presence of cobalt ions in the solution.

3.6 Effect of current density

Figure 14 shows the effect of current density on the potential. The steady state potentials were lower in the

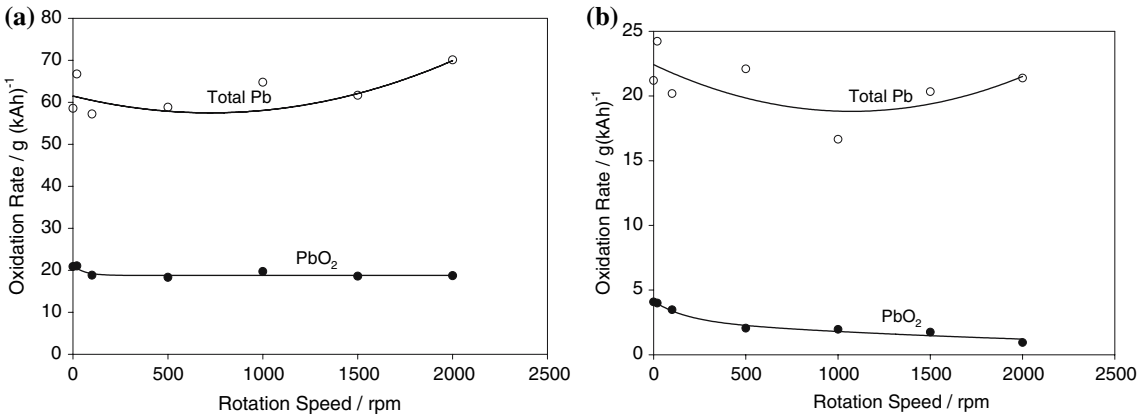

Fig. 9 The effect of rotation speed on the oxidation rate [expressed as total Pb] and the amount of PbO_2 [expressed as Pb] on the Pb–Ca–Sn alloy after oxidation for 1 h at 285 A m^{-2} in 170 g L^{-1} H_2SO_4 containing (**a**) 0 ppm Co^{2+} and (**b**) 100 ppm Co^{2+}

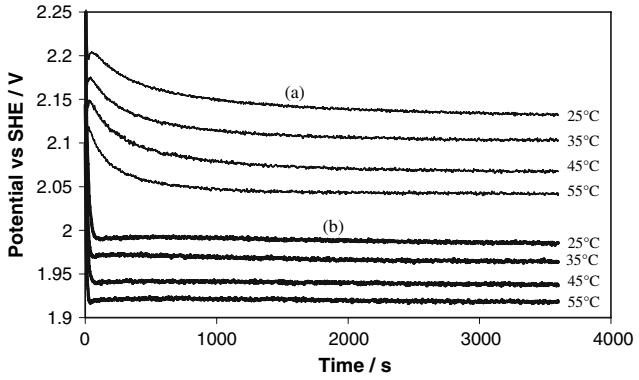

Fig. 10 Effect of temperature on the potential of the Pb–Ca–Sn alloy during oxidation at 285 A m^{-2} in 170 g L^{-1} H_2SO_4 containing (**a**) 0 ppm Co^{2+} and (**b**) 100 ppm Co^{2+}

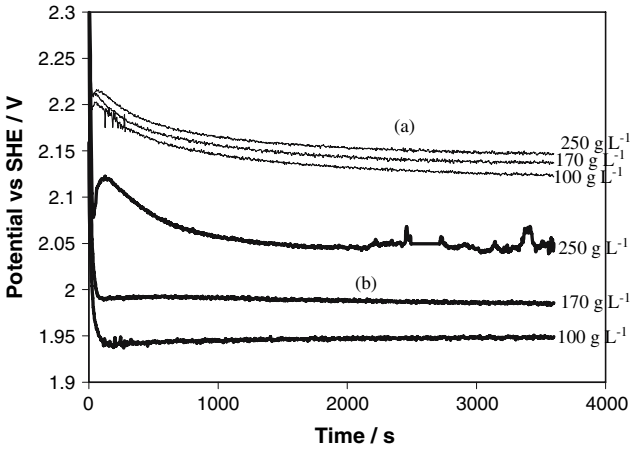

Fig. 12 Effect of acid concentration on the potential of the Pb–Ca–Sn alloy during oxidation at 285 A m^{-2} in 170 g L^{-1} H_2SO_4 containing (**a**) 0 ppm Co^{2+} and (**b**) 100 ppm Co^{2+}

presence of cobalt ions. The steady state potential increased with increased current density; this increase was smaller in the presence of cobalt ions.

Table 1 shows that an increase in current density correlated with a significantly decreased oxidation rate as well as a decrease in the amount of PbO_2. The oxidation rate and the amount of surface PbO_2 was lower in the presence of cobalt ions. This is contrary to an observation reported in the literature for a Pb–Co_3O_4 composite anode [15]. The total amount of Pb oxidised was essentially independent of the applied current density; this indicates that, as the current density was increased, a smaller fraction was associated with oxidation of the Pb–Ca–Sn alloy. If the complement of the current density is evolved in the oxygen evolution reaction, the implication is that current efficiency of the oxygen evolution reaction is greater at the higher current densities.

3.7 Oxidised Pb–Ca–Sn anode in cobalt containing solution

Figure 15 presents the potential decay transients of the Pb–Ca–Sn alloy in a 170 g L^{-1} H_2SO_4 solution with the stated cobalt ion concentration after the alloy had been oxidised for 24 h at 285 A m^{-2} in the same solution. The potential started at about 1.8–1.9 V and decayed toward a plateau at $\sim$1.6 V which can be attributed to the potential of the PbO_2/$PbSO_4$ couple.

In the absence of cobalt ions, the potential remained at the plateau at $\sim$1.6 V for $\sim$1.5 h after which the potential decreased to another plateau at about 1.1 V, where it remained for several hours before decreasing again toward the Pb/$PbSO_4$ potential (not shown on the figure).

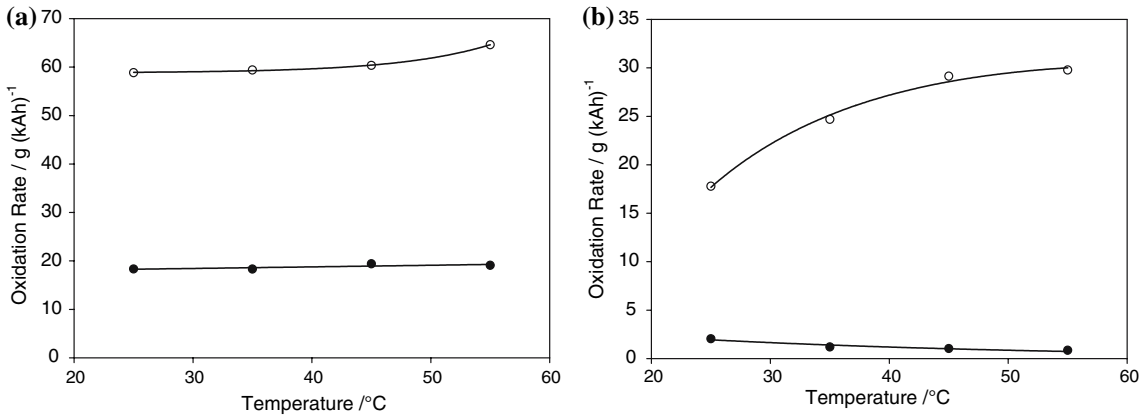

Fig. 11 Effect of temperature on the oxidation rate [expressed as total Pb] and the amount of PbO_2 [expressed as Pb] on the Pb–Ca–Sn alloy after oxidation for 1 h at 285 A m^{-2} in 170 g L^{-1} H_2SO_4 containing (**a**) 0 ppm Co^{2+} and (**b**) 100 ppm Co^{2+}

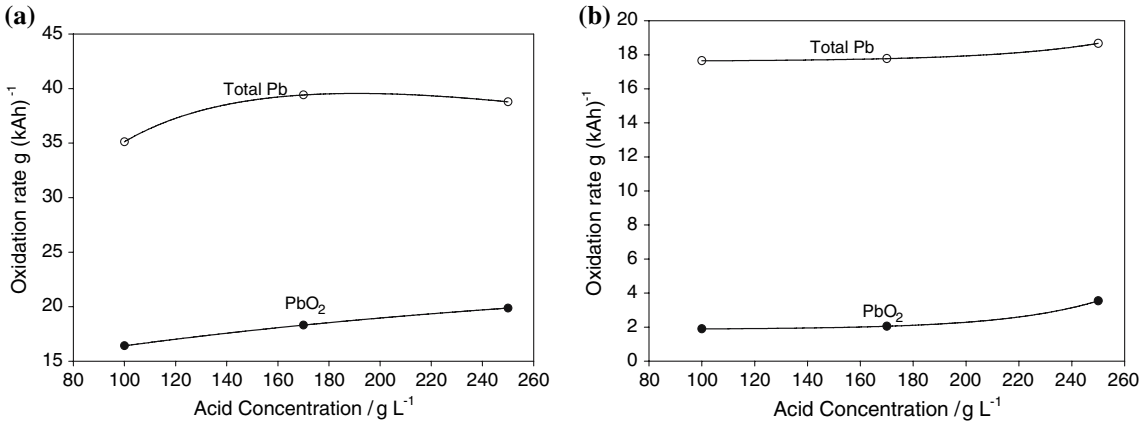

Fig. 13 Effect of acid concentration on the oxidation rate [expressed as total Pb] and the amount of PbO_2 (expressed as Pb) on the Pb–Ca–Sn alloy after oxidation for 1 h at 285 A m^{-2} in 170 g L^{-1} H_2SO_4 containing (**a**) 0 ppm Co^{2+} and (**b**) 100 ppm Co^{2+}

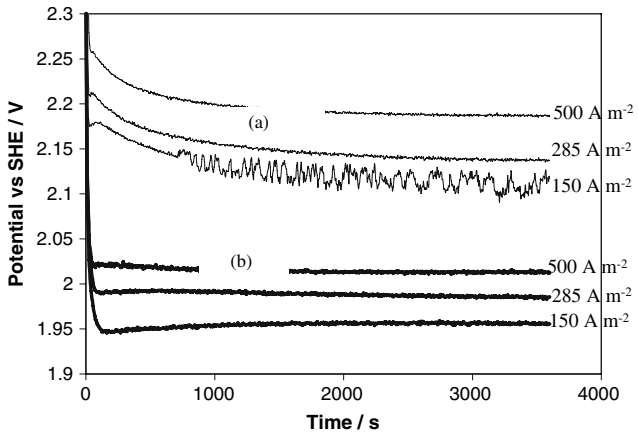

Fig. 14 Effect of current density on the potential of the Pb–Ca–Sn alloy during oxidation in 170 g L^{-1} H_2SO_4 containing (**a**) 0 ppm Co^{2+} and (**b**) 100 ppm Co^{2+}

In solutions containing cobalt ions the transients were similar. The potential decayed to the plateau at about 1.6 V and then decayed to the Pb/$PbSO_4$ potential at about –0.3 V (which is not shown for (b) in Fig. 15). In solutions containing 100 and 500 mg L^{-1} Co^{2+} (b and c) there was an intermediate plateau between 1.2 and 1.4 V. The time at the plateau at ~1.6 V decreased with increasing cobalt ion concentration.

3.8 Oxidised Pb–Ca–Sn anode in a cobalt-free solution

The Pb–Ca–Sn alloy was oxidised in a 170 g L^{-1} H_2SO_4 solution containing 500 mg L^{-1} Co^{2+} for 24 h at 285 A m^{-2}; then the alloy was transferred as quickly as possible into a cobalt-free 170 g L^{-1} H_2SO_4 solution and the potential was measured as shown in Fig. 16(a). The potential remained at the potential of the PbO_2/$PbSO_4$ couple for almost 10 h before it decreased toward the potential of the Pb/$PbSO_4$ couple. For comparison purposes, Fig. 16(b) shows the curve for an alloy that had been oxidised in 170 g L^{-1} H_2SO_4 + 500 mg L^{-1} Co^{2+} for 24 h after which the potential was measured in the same solution.

4 Discussion

4.1 Anode oxidation mechanism

The results of Sect. 3.2 indicated that the structure of the anodic film formed in solutions containing cobalt ions was thin and dense whereas the film formed in solutions with no cobalt ions was loose and porous. The total amount of oxidation, and the amount of PbO_2, decreased with increasing cobalt ion concentration in the solution. Thus,

Table 1 Effect of current density on the oxidation rate [expressed as total Pb], the amount of PbO_2 [expressed as Pb] on the Pb–Ca–Sn alloy surface and total amount of Pb oxidised, after oxidation for 1 h at 285 A m^{-2} in 170 g L^{-1} H_2SO_4 containing 0 or 100 ppm Co^{2+}

Current	170 g L^{-1} H_2SO_4 + 0 ppm Co^{2+}			170 g L^{-1} H_2SO_4 + 100 ppm Co^{2+}		
Density A m^{-2}	Total oxidation rate, g (kAh) $^{-1}$	PbO_2 g (kAh) $^{-1}$	Total Pb oxidized g/m^{-2}	Total oxidation rate, g (kAh) $^{-1}$	PbO_2 g (kAh) $^{-1}$	Total Pb oxidised g (kAh)$^{-1}$
150	–	–		35.0	3.8	5.3
285	57.4	19.2	16.4	15.6	2.0	4.4
500	32.4	12.0	16.2	8.6	1.0	4.3

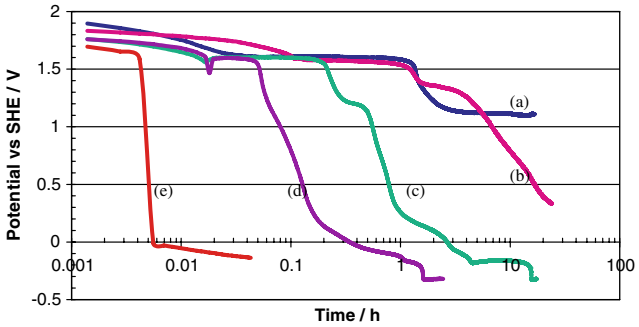

Fig. 15 The potential of the Pb–Ca–Sn alloy, after oxidation for 24 h at 285 A m^{-2}, measured in the same solution. The 170 g L^{-1} H_2SO_4 solution contained cobalt ion concentrations of (**a**) 0 mg L^{-1}, (**b**) 100 mg L^{-1}, (**c**) 500 mg L^{-1}, (**d**) 2,000 mg L^{-1} and (**e**) 5,000 mg L^{-1}

the presence of cobalt ions in the solution changed the structure, morphology and chemical composition of the surface film, from a loose porous film with a substantial PbO_2 content to a thin dense film. This change of surface film structure is interpreted as the cause of the decreased rate of oxidation for the lead anode in the cobalt ion containing solution.

The steady state potential on the Pb-Ca-Sn alloy anode decreased with (i) increasing cobalt ion concentration (Sect. 3.2), (ii) increasing rotation speed; the effect of electrode rotation speed on potential was more pronounced in the solution containing cobalt ions (Sect. 3.3), (iii) increasing temperature with lower potentials in the cobalt ion containing solutions (Sect. 3.4), (iv) decreasing acid concentration with lower potentials in the presence of cobalt ions (Sect. 3.5) and (v) decreasing current density with lower potentials in the presence of cobalt ions (Sect. 3.6).

The influence of rotation speed suggests that mass transfer at least partially controls the reaction, which is oxygen evolution by Eq. 1 in the absence of cobalt ions, Fig. 8(a). In the presence of cobalt ions (Fig. 8(b)) it may be that the key effect is that the oxygen evolution

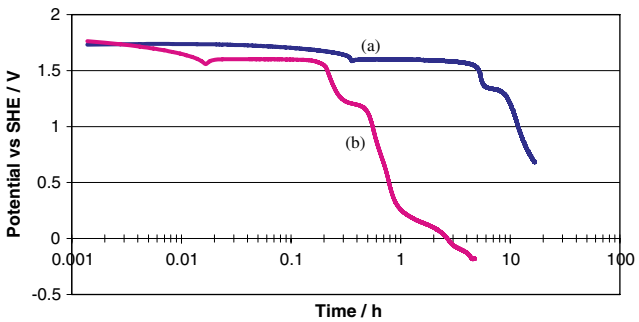

Fig. 16 Potential for the Pb–Ca–Sn alloy after oxidation in a 170 g L^{-1} H_2SO_4 solution containing 500 mg L^{-1} cobalt ions. (**a**) potential measured in a cobalt ion free solution. (**b**) potential measured in the same solution containing 500 mg L^{-1} cobalt ions

reaction is faster on the more compact film formed in the presence of cobalt ions. Alternatively, it is possible that there is sufficient current flow in the alternative pathway of oxidation of Co^{2+} by Eq. 4. Use of the Levich equation reveals that the limiting current for oxidation of cobalt(II) to cobalt(III) at a rotating (2,000 rpm) disk in a solution containing 100 mg L^{-1} cobalt ions is about 10 A m^{-2}. This is a small fraction of the total current density during oxidation and it is therefore possible that oxidation of cobalt(II) to cobalt(III) is occurring given that the standard potential for the reaction $Co^{3+} + e = Co^{2+}$ is about 1.81 V. Thus, an additional pathway for oxygen evolution involving the oxidation of water by generated cobalt(III) ions is possible as has been previously suggested [4, 5].

The oxidation rate of the Pb–Ca–Sn alloy (i) decreased with increasing cobalt ions, (ii) was largely independent of rotation speed, but lower oxidation rates were measured with cobalt ions present in, (iii) increased somewhat with increasing temperature, with lower oxidation rates measured in the presence of cobalt ions, (iv) increased with acid concentration with lower oxidation rates with cobalt ions present, and (v) decreased with increasing current density with lower oxidation rates with cobalt ions.

The results showed a decreased oxidation rate of the Pb–Ca–Sn alloy in the presence of cobalt ions. This decrease in oxidation rate is consistent with the lower potential providing a lower driving force for lead oxidation. However, this possible explanation is not consistent with the data of Table 1 which show that the total amount of Pb oxidised did not change with increasing applied current density. This decrease in the oxidation rate was consistent with the formation of a more dense and protective surface film. There is thus a strong case that the lower oxidation rate of the lead alloy in the presence of the cobalt ions is caused by a more compact film. This would be consistent with many other situations [24–32]. There is no particular reason for there to be a cobalt surface film as previously postulated [3], but on the other hand, there is nothing in the present experimental results that can exclude the presence of a surface cobalt film.

This conclusion from the laboratory studies is that the lower oxidation rate in the presence of the cobalt ions is caused by the more compact surface film. It is expected that this conclusion would be equally valid for plant conditions.

4.2 Potential transients

Figure 15 presents the potential transients for a freshly polished Pb–Ca–Sn electrode after oxidation at a current density of 285 A m^{-2} in a 170 g L^{-1} H_2SO_4 solution. During

oxidation, the surface of the Pb–Ca–Sn is oxidised to PbO_2. When the oxidising current is switched off, the lead dioxide transforms to lead sulphate because thermodynamically lead dioxide is unstable on the surface of lead in the sulphuric acid solutions. At the surface of the film at the electrolyte, PbO_2 is electrochemically reduced (see cathodic peak C in Fig. 3) according to the following reaction

$$PbO_2 + HSO_4^- + 3H^+ + 2e^- \rightarrow PbSO_4 + 2H_2O \quad E^\circ = 1.685V \tag{7}$$

The time for which the potential remained at plateau at ~ 1.6 V is a measure of the time taken to convert the PbO_2 to $PbSO_4$. This time relates to the amount of PbO_2 present as well as to the difficulty of converting the PbO_2 into $PbSO_4$. Assuming the form of the PbO_2 was the same in all cases, the shorter time at 1.6 V implies that there was a smaller amount of surface PbO_2 with increasing cobalt ion concentration, which is consistent with the prior results. The origin of the second plateau at about 1.1 V may be associated with the reduction of PbO_2 to form basic lead sulphate [33]:

$$2PbO_2 + HSO_4^- + 5H^+ + 4e^- \rightarrow PbO \cdot PbSO_4 + 3H_2O \quad E^\circ = 1.375V \tag{8}$$

Figure 16(a) shows that the potential remained at the $PbO_2/PbSO_4$ potential for almost 10 h for the Pb–Ca–Sn electrode oxidised in the 170 g L^{-1} H_2SO_4 solution containing 500 mg L^{-1} Co^{2+} for 24 h at 285 A m^{-2} and then open-circuited in the cobalt-free 170 g L^{-1} H_2SO_4 solution. In comparison Fig. 16(b) shows that the free corrosion potential remained at the $PbO_2/PbSO_4$ potential for only half an hour after oxidation under the same conditions if the electrode was open-circuited in the same cobalt containing solution (170 g L^{-1} H_2SO_4 + 500 mg L^{-1} Co^{2+}). Thus, the presence of cobalt ions appears to enhance the rate of reduction of the PbO_2 surface layer. This could be due to partial reduction of PbO_2 by cobalt(II) ions to form cobalt(III) ions which is thermodynamically possible for the activity ratio $Co(III)/Co(II) < 0.01$.

Each of the potential decay experiments indicated that that there was no permanency for the anode regarding subsequent dissolution of the surface oxide produced during oxidation of the lead anode.

5 Conclusions

Cobalt ions in the solution changed the structure, morphology and chemical composition of the surface film, from a loose porous film with a substantial PbO_2 content, to a thin dense film. This change of surface film structure is the cause of the decreased rate of oxidation for the lead anode in the cobalt ion containing solution. It is expected that this conclusion from the laboratory studies would be equally valid for plant conditions.

The steady state potential of the Pb-Ca-Sn alloy during oxidation with applied current decreased with (i) increasing cobalt ion concentration, (ii) increasing rotation speed, (iii) increasing temperature, (iv) decreasing acid concentration and (v) decreasing current density. In all cases the potentials were lower in the presence of cobalt ions. The potential of the anode is largely controlled by the oxygen evolution reaction. The results indicate that this oxygen evolution reaction is faster on the more compact film formed in the presence of cobalt ions, and that the reaction rate is increased in the presence of cobalt ions. Alternatively, the lower potential values may be due to the existence of an alternative pathway of oxidation provided by the Co^{2+}/Co^{3+} couple in.

The oxidation rate decreased with increasing cobalt ions and in all cases studied lower oxidation rates were measured with cobalt ions present.

The amount of lead oxidized was independent of anodic current density indicating that mechanisms based on a reduced potential are not applicable to lead oxidation under conditions of electro-winning.

The free corrosion potential decay curves were consistent with a lower amount of PbO_2 on the surface after oxidation in a cobalt ion containing solution.

Acknowledgements The authors thank the Amira Project P705, the AJ Parker CRC and The University of Queensland for support.

References

1. Rey M, Coheur P, Herbiet H (1938) Trans Amer Electrochem Soc 73:315
2. Koenig AE, MacEwan JU, Larsen EC (1941) Trans Amer Electrochem Soc 79:331
3. Krivolapova EV, Kabanov BN (1950) Trudy Soveshchaniya Elektrokhim Akad Nauk SSSR, 539
4. Koch DFA (1959) Aust J Chem 12:127
5. Antonov SP, Stepanenko VG (1972) Ukr Khim Zh 38:935
6. Gendron AS, Ettel VA, Abe S (1975) Can Metall Q 14:59
7. Nidola A (1989) Mater Chem Phys 22:183
8. Bagshaw NE (1997) J Power Sources 64:91
9. Cachet C, Le Pape-rérolle C, Wiart R (1999) J Appl Electrochem 29:811
10. Prengaman RD, Siegmund A (1999) In: Dutrizac JE, Ji J, Ramachandran V (eds) Proceedings of international conference copper 99, The Minerals, Metals & Materials Society, Phoenix, Arizona, USA
11. Rashkov S, Dobrev T, Noncheva Z, Stefanov Rashkova YB, Petrova M (1999) Hydrometallurgy 52:223
12. Yu P, O'Keefe JO (1999) J Electrochem Soc 146:1361

13. Branzoi V, Branzoi F, Trimbitasu E, Pilan L (2001) UPB Sci Bull Ser B 63:9
14. Hrussanova A, Mirkova L, Dobrev T (2001) Hydrometallurgy 60:199
15. Hrussanova A, Mirkova L, Dobrev T, Vasilev S (2004) Hydrometallurgy 72:205
16. Hrussanova A, Mirkova L, Dobrev T, Vasilev S (2004) Hydrometallurgy 72:215
17. Kittelty D (2004) Amira P705 project progress report. AJ Parker CRC for Hydrometallurgy, Perth, WA
18. Panda B, Das SC, Panda RK (2004) Hydrometallurgy 72:149
19. Pagliero A, Vergara F, Delplancke JL, Winand R (1999) In: Dutrizac JE, Ji J, Ramachandran V (eds) Proceedings international conference copper 99, The Minerals, Metals & Materials Society, Phoenix, Arizona, USA
20. Czerwinski A, Zelazowska M, Grden M, Kuc K, Milewski JD, Nowacki A, Wojcik G, Kopczyk M (2000) J Power Sources 85:49
21. Paleska I, Pruszkowska R, Kotowski J, Dziudzi A, Milewski JD, Kopczyk M, Czerwinski A (2003) J Power Sources 113:308
22. Rus EM, Taralunga G (2001) UPB Sci Bull Ser B 63:513
23. Velichenko AB, Amadelli R, Baranova EA, Girenko DV, Danilov FI (2002) J Electroanal Chem 527:56
24. Bruesch P, Muller K, Atrens A, Neff H (1985) Appl Phys A 38:1–18
25. Jin S, Atrens A (1987) Appl Phys A 42:149–65
26. Jin S, Atrens A (1990) Appl Phys A 50:287–300
27. Lim AS ,Atrens A (1991) Appl Phys A 53:273–281
28. Lim AS, Atrens A (1992) Appl Phys A 54:500–507
29. Atrens A, Baroux B, Mantel M (1997) J Electrochem Soc 144:3697–3704
30. FitzGerald KP, Nairn J, Atrens A (1998) Corrosion Sci 40:2029–2050
31. Song GL, Atrens A, Wu X, Zhang B (1998) Corrosion Sci 40:1769–1791
32. FitzGerald KP, Nairn J, Skennerton G, Atrens A (2006) Corrosion Sci 48:2480–2509
33. Ruetschi P, Angstadt RT (1964) J Electrochem Soc 111:1323